THE JOURNAL OF BIOLOGICAL CHEMISTRY VOL. 288, NO. 42, pp. 30571–30584, October 18, 2013

Membrane Vesicles Nucleate Mineralo-organic Nanoparticles and Induce Carbonate Apatite Precipitation in Human Body Fluids*

Received for publication, June 9, 2013, and in revised form, August 28, 2013 Published, JBC Papers in Press, August 29, 2013, DOI 10.1074/jbc.M113.492157

Cheng-Yeu Wu[‡§¶1], **Jan Martel**[‡§1], **Wei-Yun Cheng**[‡§], **Chao-Chih He**[‡§], **David M. Ojcius**[§‖], **and John D. Young**[‡§**‡‡2]

From the [‡]*Laboratory of Nanomaterials, the* [§]*Center for Molecular and Clinical Immunology, and the* [¶]*Research Center of Bacterial Pathogenesis, Chang Gung University, Gueishan, Taoyuan 333, Taiwan, the* [‖]*Molecular Cell Biology, Health Sciences Research Institute, University of California, Merced, California 95343, the* [**]*Laboratory of Cellular Physiology and Immunology, Rockefeller University, New York, New York 10021, and the* [‡‡]*Biochemical Engineering Research Center, Ming Chi University of Technology, Taishan, Taipei 24301, Taiwan*

Background: Membrane vesicles (MVs) released from various cells are associated with human diseases.
Results: MVs isolated from human serum induce the formation of mineralo-organic nanoparticles in culture.
Conclusion: MVs represent a nucleating factor that promotes the formation of mineralo-organic nanoparticles and the precipitation of mineral deposits in body fluids.
Significance: The ectopic precipitation of carbonate apatite deposits in body fluids and tissues may be initiated in part by MVs.

Recent studies indicate that membrane vesicles (MVs) secreted by various cells are associated with human diseases, including arthritis, atherosclerosis, cancer, and chronic kidney disease. The possibility that MVs may induce the formation of mineralo-organic nanoparticles (NPs) and ectopic calcification has not been investigated so far. Here, we isolated MVs ranging in size between 20 and 400 nm from human serum and FBS using ultracentrifugation and sucrose gradient centrifugation. The MV preparations consisted of phospholipid-bound vesicles containing the serum proteins albumin, fetuin-A, and apolipoprotein A1; the mineralization-associated enzyme alkaline phosphatase; and the exosome proteins TNFR1 and CD63. Notably, we observed that MVs induced mineral precipitation following inoculation and incubation in cell culture medium. The mineral precipitates consisted of round, mineralo-organic NPs containing carbonate hydroxyapatite, similar to previous descriptions of the so-called nanobacteria. Annexin V-immunogold staining revealed that the calcium-binding lipid phosphatidylserine (PS) was exposed on the external surface of serum MVs. Treatment of MVs with an anti-PS antibody significantly decreased their mineral seeding activity, suggesting that PS may provide nucleating sites for calcium phosphate deposition on the vesicles. These results indicate that MVs may represent nucleating agents that induce the formation of mineral NPs in body fluids. Given that mineralo-organic NPs represent precursors of calcification *in vivo*, our results suggest that MVs may initiate ectopic calcification in the human body.

Recent studies indicate that various NPs[3] present in the environment constantly interact with the human body and may be associated with disease conditions. For instance, the inhalation of asbestos nanofibers derived from fireproof materials is associated with the development of lung cancer and fibrotic lung damage known as asbestosis (1). Similarly, titanium dioxide NPs, which are widely used as whitening agents in commercial products, induce acute toxicity to various organs in laboratory animals (2). Given that NPs show unexpected size-dependent properties and increased access to various body compartments, the potential toxicity of such nanomaterials represents an important safety concern and is now a major research focus in the fields of nanomedicine and nanotoxicology (3).

Mineralized NPs called NB were initially described as the smallest living microorganisms on earth (4) and as the possible causative agent of various human diseases, including Alzheimer disease, atherosclerosis, cancer, chronic kidney disease, kidney stones, and prostatitis (5–7). However, recent studies performed by us (8–17) and others (18–22) have shown that the so-called NB actually represent non-living mineralo-organic NPs that possess biomimetic properties, including the ability to increase in size and number in culture. Although the hypothesis that NB represent living microorganisms has been discarded, several studies have indicated that mineral NPs similar to NB do form in the growing bones and teeth of vertebrates (23–25). Mineralo-organic NPs have also been observed in undesired, ectopic calcification associated with various human and animal conditions (26–30). As such, these mineral NPs may represent calcification precursors found in both physiological and pathological mineralization processes.

* This work was supported by the Primordia Institute of New Sciences and Medicine and Chang Gung University Grant QZRPD88E; Ming Chi University of Technology Grant 0XB0; Ministry of Education of Taiwan, Republic of China, Grant EMRPD1B0471; and National Science Council of Taiwan Grant 101-2632-B-182-001-MY3.
[1] Both authors contributed equally to this work.
[2] To whom correspondence should be addressed: Laboratory of Nanomaterials, Chang Gung University, Gueishan, Taoyuan 333, Taiwan, Republic of China. Tel.: 886-3211-8800 (ext. 3772); Fax: 886-3211-8534; E-mail: dingeyoung@hotmail.com.

[3] The abbreviations used are: NP, nanoparticle; ALP, alkaline phosphatase; apoA-I, apolipoprotein AI; CPP, calciprotein particle; DiR, 1,1′-dioctadecyl-3,3,3′,3′-tetramethylindotricarbocyanine iodide; EDX, energy-dispersive x-ray; HAP, hydroxyapatite; HS, human serum; MV, membrane vesicle; NB, nanobacteria; PS, phosphatidylserine; TEM, transmission electron microscopy; VSMC, vascular smooth muscle cell.

Human body fluids have been shown to contain membrane vesicles (MVs) in the form of small lipid-bound vesicles released from various cells (31). These vesicles have been broadly categorized as exosomes, microvesicles, and apoptotic bodies (32). Exosomes represent 30–100-nm vesicles released from cellular endosomes and are thought to be involved in cell-to-cell signaling (32–34). Microvesicles are a more heterogeneous group of 100–1,000 nm vesicles released from the plasma membrane of various cells; they have been implicated in intercellular communication, homeostasis, and cellular waste disposal (32, 35). Apoptotic bodies represent particles ranging from 50 nm to 5 μm, which are released by apoptotic cells and removed through phagocytosis by macrophages (32, 34). Given that the level of MVs is elevated in the body fluids of humans afflicted with various ailments, some authors have proposed that these vesicles may play a role in disease conditions that include arthritis, atherosclerosis, cancer, and chronic kidney disease (31, 36, 37). On the other hand, it remains unclear whether MVs represent a consequence of the disease process or whether they play an active role in pathogenesis.

Matrix vesicles represent a different type of extracellular vesicles implicated in physiological and pathological calcification processes in vertebrates (38–40). Matrix vesicles are 20–200-nm vesicles released from mineralizing cells, such as osteoblasts and odontoblasts, which induce mineralization in bones and teeth, respectively. During ectopic vascular calcification, these vesicles are also released by vascular smooth muscle cells (VSMCs), which develop into osteoblast-like cells and induce calcium phosphate precipitation when exposed to excess phosphate, inflammation, or hyperlipidemia (38–40). Matrix vesicles are thought to induce mineralization by concentrating calcium and phosphate ions in various ways, including via specific ion transporters; in addition, these vesicles contain enzymes, such as alkaline phosphatase (ALP), which degrades calcification inhibitors (*e.g.* pyrophosphate) and releases phosphate from various organic molecules. Although MVs similar to matrix vesicles and apoptotic bodies have been repeatedly described in calcified tissues (30, 41), the possibility that such vesicles may induce the formation of mineralo-organic NPs in body fluids has not been investigated.

Phosphatidylserine (PS), a phospholipid usually confined to the inner lipid layer of the cell membrane (42), has been found on the surface of various populations of MVs (32, 40). When present on platelet-derived microvesicles, PS induces blood coagulation, a phenomenon associated with an increased risk of thrombosis (42, 43). On the surface of apoptotic bodies, PS is thought to represent a signal that induces phagocytosis and clearance of the vesicles by macrophages (42). Notably, PS possesses calcium-binding properties and may provide a nucleating site for calcium phosphate formation on both matrix vesicles (38–40) and apoptotic bodies (44). Whether PS found on the surface of MVs may induce the mineralization of MVs in body fluids remains to be examined.

Several studies have been conducted to identify the factors that induce formation of the so-called NB and mineralo-organic NPs. Cisar *et al.* (18) observed that the cell membrane lipid phosphatidylinositol produces mineral NPs similar to NB after inoculation in DMEM and incubation in cell culture conditions. Raoult *et al.* (22) speculated that fetuin-A, a systemic calcification inhibitor (45, 46) associated with NB (9, 22), may initially inhibit NB formation but eventually act as a nucleator of NB formation following a conformational change similar to prion conversion. Our own experiments have shown that serum proteins like albumin and fetuin-A fail to induce NB formation under the conditions tested, although these proteins may form seeds for the formation of mineralo-organic NPs once the concentrations of calcium and phosphate ions exceed saturation (11). These results suggest that other molecules or structures, possibly in the form of lipid membranes, may represent factors that induce the formation of mineralo-organic NPs similar to the so-called NB in body fluids.

In the present study, we examined the possibility that mineral NP formation may be induced by MVs present in body fluids. We isolated a population of MVs from human serum (HS) and FBS and characterized the morphological and biochemical composition of these particles. Our results show that the isolated serum MVs induce the formation of mineralo-organic NPs when inoculated and incubated in cell culture medium, suggesting that MVs may serve as a nucleating agent of mineral NPs in culture and as a factor that induces ectopic calcification in human body fluids.

MATERIALS AND METHODS

Isolation of Membrane Vesicles—Blood was collected from healthy human volunteers using a conventional venipuncture method. Written informed consents were obtained from the volunteers, and the use of human samples was approved by the Institutional Review Board of Chang Gung Memorial Hospital (Linkou, Taiwan). Whole blood was collected into Vacutainer tubes without anticoagulant (BD Biosciences). After centrifugation at 1,500 × *g* for 15 min at room temperature, the supernatant corresponding to HS was collected and stored at −20 °C. HS and commercial FBS (Biological Industries) were filtered through 0.2-μm pore membranes prior to use.

MVs were isolated as before (47, 48), with minor modifications. Briefly, 10 ml of HS and FBS was centrifuged at 800 × *g* for 15 min at 4 °C to spin down and remove large cell debris. The resulting supernatant was centrifuged for 30 min at 10,000 × *g*. The supernatant obtained this way was centrifuged for 60 min at 15,000 × *g* (SW27 rotor, Beckman Instruments). Material present in the supernatant was pelleted by ultracentrifugation at 200,000 × *g* for 2 h at 4 °C (SW41 rotor, Beckman Instruments). The pellet was suspended in 1 ml of HEPES buffer (20 mM HEPES, 140 mM NaCl, pH 7.4) and is referred in the present study as "membrane vesicles" (MVs). In some experiments, sodium azide was added at 0.02% to prevent microbial contamination.

Dynamic Light Scattering—One ml of resuspended MVs was transferred to disposable plastic cuvettes (Kartell) and mixed by gentle inversion prior to reading using a Delsa Nano Submicron Particle Analyzer (Beckman Coulter). Measurements were performed at room temperature at an incident angle of 165°. Although the relative particle unit used in the *y* axis of Fig. 1, *A* and *B*, represents arbitrary values, this unit correlates in a linear manner with the observed particle amount under the conditions used.

Optical and Electron Microscopies—Aliquots of MVs resuspended in HEPES buffer were deposited on glass slides and observed without fixation or staining with a BX-51 optical microscope (Olympus) equipped with a ×100 oil immersion objective with iris (UPlanFLN, Olympus) and a dark field condenser (Cerbe Distribution). Specimens were observed at a magnification of ×1,000, and images were acquired with a Spot Flex color camera (Diagnostic Instruments).

For negative stain TEM, MV preparations were deposited onto Formvar carbon-coated grids and negatively stained with 0.5% aqueous uranyl acetate, followed by drying overnight at room temperature. In some experiments, MVs were treated with 0.1% (v/v) Triton X-100 prior to processing for negative staining. Specimens were examined under an EMU-3C (RCA) or JEM-100B (JEOL) transmission electron microscope.

Precipitates obtained following incubation of DMEM containing MVs (with or without added serum) were pelleted by centrifugation at 12,000 × *g* for 15 min and washed twice with HEPES buffer prior to resuspension in the same buffer. A small aliquot was deposited onto carbon-coated grids before drying overnight. In this case, the particles were observed without fixation or staining by TEM. Electron diffraction patterns were obtained with the JEM-100B transmission electron microscope operated at 120 keV.

For immunogold staining, MVs were deposited onto nickel grids and blocked with PBS plus 1% gelatin. The grids were placed on liquid drops containing the diluted protein or antibody for 1 h at room temperature. MVs were treated successively with annexin V (BD Biosciences), rabbit polyclonal anti-annexin V antibody (sc-8300, Santa Cruz Biotechnology, Inc.), and goat anti-rabbit antibody conjugated with a 5-nm gold NP (R-14001, Agar Scientific). Between each treatment, MVs were washed successively with PBST, 0.1% Tween 20 in PBS (5 min).

Fluorescence Spectroscopy—MVs were quantified as before (49, 50) by measuring the concentration of total proteins using a commercial Bradford protein assay (Bio-Rad). To detect lipid membranes, we mixed a fraction of MVs corresponding to 0.5 μg of MV proteins with 0.1 mM 1,1′-dioctadecyl-3,3,3′,3′-tetramethylindotricarbocyanine iodide (DiR; Molecular Probes) in a final volume of 1 ml. The probe was initially dissolved in 0.5% ethanol. Specimens were incubated for 1 h at room temperature with continuous agitation. The same amount of lipophilic tracer was added to HEPES buffer and processed in the same manner as a negative control. THP-1 cells (2×10^4 cells/ml) purchased from the American Type Culture Collection (ATCC) were used as a positive control. These cells were maintained in RPMI 1640 medium containing 10% FBS and 100 units/ml of both penicillin and streptomycin. Fluorescence was measured using a fluorescence microplate reader (Spectra Max M5 Spectrophotometer, Molecular Devices) with excitation at 748 nm and emission at 780 nm.

To detect PS on the surface of MVs, we mixed 5 μl of FITC-labeled annexin V (BD Biosciences) with a MV fraction corresponding to 30 μg of total MV proteins dissolved in 100 μl of HEPES buffer (containing 2.5 mM $CaCl_2$), with or without 0.5 mM EDTA. Reaction mixtures were incubated for 30 min at room temperature and subsequently washed with HEPES buffer to remove unbound annexin V following ultracentrifugation at 200,000 × *g*. Fluorescence emission was measured at 535 nm following excitation at 485 nm.

Sucrose Gradient Centrifugation—MV preparations obtained by ultracentrifugation were diluted to 10% (v/v) in 1 ml of HEPES buffer and layered on top of a centrifugation tube (Ultra-Clear centrifugation tubes, 14 × 89 mm, Beckman Instruments) containing a linear sucrose gradient (0.2–20% sucrose, 20 mM HEPES, pH 7.4) prepared using a gradient maker (Gradient Station, BioComp Instruments). After centrifugation at 100,000 × *g* for 15 h at 4 °C, 1-ml fractions were collected from the top of the tube. Collected fractions were dialyzed using a commercial microdialysis system (Invitrogen) using a membrane with a 12–14-kDa cut-off (Spectra).

Lipid Analysis—Lipids were quantified in sucrose gradient fractions by using commercial kits for phospholipids (BioAssay Systems), cholesterol, triglycerides, HDL, and LDL (BioVision) based on the manufacturer's instructions.

Western Blotting—SDS-PAGE and Western blot analysis were performed as before (9). A fraction of MVs corresponding to 60 μg of MV proteins, 60 μg of proteins from mineralo-organic NPs seeded by MVs, or 60 μg of proteins from either HeLa cells or whole serum was dissolved in 5× "loading buffer" (0.313 M Tris-HCl, pH 6.8, 10% SDS, 0.05% bromophenol blue, 50% glycerol, 12.5% β-mercaptoethanol) to a final concentration of 1×, prior to heating at 95 °C for 5 min and separation under denaturing and reducing conditions on 10% SDS-PAGE using a minigel system (Hoefer). HeLa cells were purchased from the ATCC and cultured in minimum essential medium containing 10% FBS and 100 units/ml of both penicillin and streptomycin. The primary antibodies used were goat polyclonal anti-tissue nonspecific ALP (sc-15065, Santa Cruz Biotechnology), mouse monoclonal anti-LAMP2 (lysosome-associated membrane protein 2) (sc-18822), goat polyclonal anti-human TNFR1 (tumor necrosis factor receptor 1) (sc-31349), rabbit polyclonal anti-annexin V (sc-8300), goat polyclonal anti-CD63 (cluster of differentiation 63) (sc-31214), and rabbit polyclonal antibodies prepared in-house as described below. The secondary antibodies used were horseradish peroxidase-conjugated anti-goat, anti-mouse, anti-sheep, or anti-rabbit antibodies (Santa Cruz Biotechnology). Primary and secondary antibodies were diluted based on the instructions provided by the manufacturer. The polyclonal antibodies generated in house were used at a dilution of 1:1,000. The blots were revealed using enhanced chemiluminescence (Amersham Biosciences) and autoradiographic films (Molecular Technologies). Membranes were stripped by using the ReBlot Western blot recycling kit (Chemicon).

Production of Polyclonal Antibodies—New Zealand White rabbits were obtained at ~12 weeks of age. Human serum albumin, human serum fetuin-A, and human apolipoprotein AI (apoA-I) as well as bovine serum fetuin-A and bovine serum albumin were purchased from Sigma. The purified proteins (500 μg) were dissolved in 1 ml of DMEM and mixed with 1 ml of Freund's complete adjuvant (Sigma) using two syringes connected by a 3-way stopcock (Nipro). Each protein-adjuvant mixture was administered intradermally on the back of the animals. Three weeks after the first immunization, one booster dose (200 μg of protein in a 1:1 mixture of DMEM and incom-

plete Freund's adjuvant; Sigma) was administered every month for a total of four times. Pre- and postimmunization blood was collected from the ear vein. For apoA-I, 28–30 kDa gel bands corresponding to ~200 μg of protein from SDS-PAGE bands of whole serum were used for the immunizations as described above.

Seeding of Mineralo-organic NPs by MVs—MVs obtained by either ultracentrifugation or sucrose gradient centrifugation were added into DMEM with or without 10% serum to obtain a final volume of 1 ml. The 24-well plates were incubated under cell culture conditions in a humidified cell culture incubator at 37 °C with 5% CO_2. Photography of the plates and A_{650} readings were performed as before (9). Day 0 pictures and turbidity measurements were taken after reagent mixing. Mineralo-organic NPs obtained after incubation were pelleted by centrifugation at 12,000 × *g* for 30 min and washed twice with HEPES buffer prior to resuspension in the same buffer for further morphological and spectroscopy analyses.

Calcium Deposition Assay—The ability of MVs to calcify was assessed using a non-radioactive calcium phosphate deposition assay (49). Briefly, phospholipid-rich MV fractions corresponding to 30 μg of total MV proteins were added into DMEM and incubated in cell culture conditions. The incubation was terminated at each time point by centrifugation at 12,000 × *g* for 30 min to obtain a co-precipitate of MVs and mineralo-organic NPs. The mineral precipitate was solubilized in 0.6 M HCl for 24 h. The calcium content of the HCl supernatant was then determined colorimetrically by using the *O*-cresolphthalein complexone method (BioVision). Briefly, 2 μl of acidified supernatant was incubated for 1 min with 150 μl of calcium working reagent (chromogenic + base reagent mix) prior to measurement with a microplate spectrophotometer. Absorbance was read against a blank at 575 nm within 10 min of reagent mixing.

To evaluate the contribution of PS to mineral seeding, we mixed MVs (2 mg of total proteins) with 0.2 μg of either anti-PS or anti-CD63 antibody in a final volume of 1 ml of HEPES buffer and incubated the resulting solution for 1 h at room temperature with gentle mixing. MVs were pelleted and washed following ultracentrifugation at 200,000 × *g* for 2 h at 4 °C. MVs were resuspended and incubated in 1 ml of DMEM in cell culture conditions. After 1 week of incubation, mineral pellets were retrieved and washed using centrifugation at 12,000 × *g* for 15 min. The calcium deposition assay was used to measure the level of mineral precipitate formed.

MV Co-Precipitation Assay—A MV fraction corresponding to 30 μg of MV proteins was added into DMEM prior to the addition of 0.1–3 mM $CaCl_2$ and NaH_2PO_4 each. After incubation in cell culture conditions for 24 h, the precipitate was harvested by centrifugation at 12,000 × *g* for 30 min. After washing in HEPES buffer, the precipitate was resuspended in 50 μl of HEPES buffer and subjected to SDS-PAGE and Western blotting with the indicated antibodies. Samples that were not incubated were used in parallel for comparison.

Spectroscopy Analyses—Energy-dispersive x-ray spectroscopy (EDX) was performed as described previously (10). Briefly, material obtained after incubation of DMEM containing MVs (with or without serum) was pelleted by centrifugation at 12,000 × *g* for 30 min and washed twice with HEPES buffer prior to resuspension in water. Mineralo-organic NPs were dried overnight, and EDX spectra were acquired with an SEM S-3000N scanning electron microscope (Hitachi Science Systems) equipped with an EMAX Energy EX-400 EDX device (Horiba).

Fourier transform infrared spectroscopy (FTIR) was performed as before (11). Briefly, the spectra were acquired using a Nicolet 5700 FTIR spectrometer (Thermo Fisher Scientific) equipped with a deuterated triglycine sulfate detector. Mineralo-organic NPs were prepared by adding 1 mM $CaCl_2$ and NaH_2PO_4 each in 5% FBS, followed by incubation for 1 week in cell culture conditions (Fig. 4*D*, *FBS-NPs*). The particles were collected by centrifugation at 12,000 × *g* for 15 min and washed twice with HEPES buffer prior to drying overnight at room temperature. Commercial $CaCO_3$ (Mallinckrodt Baker), $Ca_3(PO_4)_2$ tribasic (Kanto Chemical) and HAP (buffered aqueous suspension, 25% solid; Sigma) were used for comparison.

Statistical Analysis—All experiments were performed in triplicate. The values shown represent means ± S.E. Comparisons between control and experimental groups were performed using Student's *t* test.

RESULTS

Isolation of Lipid-containing MVs from Serum—Mineralo-organic NPs initially described as NB have been shown to form when serum or other body fluids are inoculated into a cell culture medium and incubated in culture conditions for several days (4, 5). In contrast, incubation of the cell culture medium alone failed to produce mineral NPs, suggesting that nucleating agents exist in serum and body fluids. To verify whether MVs may represent a nucleating agent that induces the formation of mineralo-organic NPs in body fluids, we first isolated MVs from serum using an established protocol (see "Materials and Methods"). We hypothesized that MVs may induce mineral nucleation on their surface and thus become the core of mineralo-organic NPs. Given that mineralo-organic NPs and the so-called NB have sizes ranging from 50 to 500 nm (5, 9), we focused our attention on the smallest MVs present in body fluids and used a protocol involving ultracentrifugation to obtain vesicles with diameters below 100 nm.

After ultracentrifugation of serum, we obtained a pellet containing small, round particles of variable sizes when observed under optical, dark field microscopy (Fig. 1, *A* and *B*, *insets*). Based on dynamic light scattering analysis, the particles derived from HS showed a peak size of 37 ± 14 nm, whereas the particles obtained from FBS peaked at 28 ± 3 nm (Fig. 1, *A* and *B*). The sizes of the particles obtained were relatively heterogeneous; polydispersity index values of 0.29 and 0.22 were obtained for HS-MVs and FBS-MVs, respectively, indicating that the sizes of HS particles were more heterogeneous than for FBS particles.

Under negative stain TEM, MV preparations consisted of round particles with sizes ranging from 20 to 400 nm (Fig. 1*C*, *Control*). In order to determine whether these particles were delineated by a lipid membrane, we treated the MV preparations with Triton X-100, a non-ionic detergent with lipid-dispersing properties (48, 51). This treatment destroyed the

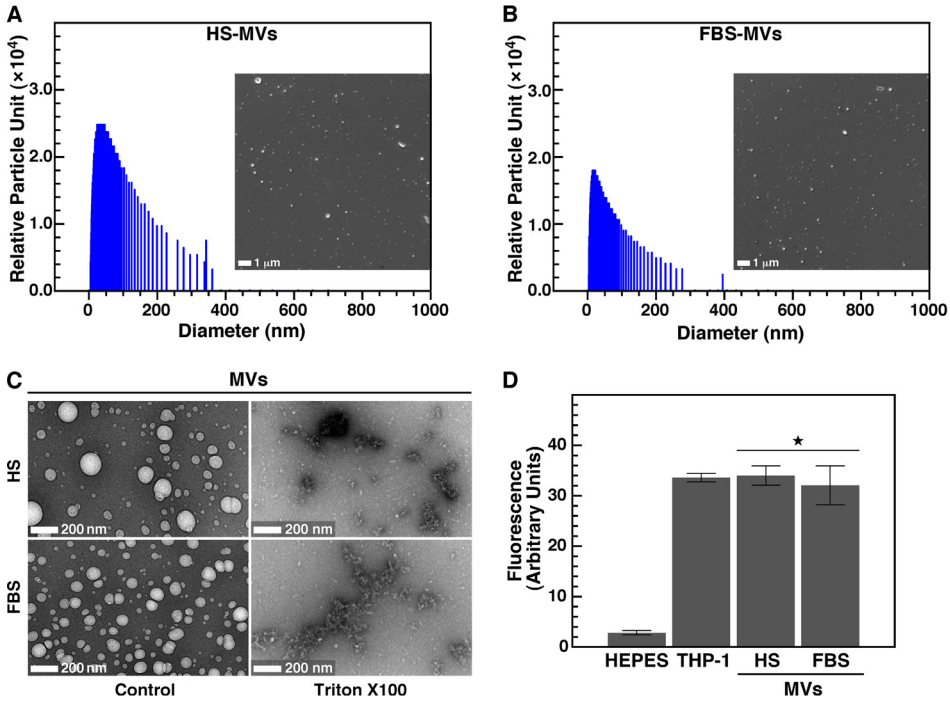

FIGURE 1. **Characterization of serum MVs isolated by ultracentrifugation.** MVs were isolated from HS (*A*) and FBS (*B*) by ultracentrifugation as described under "Materials and Methods." Round particles of heterogeneous sizes were observed under optical, dark field microscopy without fixation or staining (*insets*, ×1,000). Particle sizes measured by dynamic light scattering peaked at 37 ± 14 nm for HS and 28 ± 3 nm for FBS. *C*, negative stain TEM revealed round, 20–500-nm structures (*Control*) susceptible to treatment with a lipid-dispersing detergent (Triton X-100; 0.1%, v/v). *D*, treatment with a fluorescent, lipophilic probe (DiR; 0.1 mM) showed that both HS-MVs and FBS-MVs (corresponding to 0.5 μg of total MV proteins) produced fluorescence and thus harbored a lipid membrane. As controls, DiR produced no fluorescence in HEPES buffer but fluoresced when incorporated in cell membranes (THP-1; 2×10^4 cells/ml). *, $p <$ 0.01 *versus* control HEPES. *Error bars*, S.E.

integrity of serum-derived particles, leaving only membrane remnants (Fig. 1*C*, *Triton X-100*). To confirm these observations, we used the lipophilic tracer DiR, which is weakly fluorescent in an aqueous environment but becomes highly fluorescent when intercalated within a lipid membrane. Accordingly, DiR did not fluoresce in HEPES buffer used as a negative control but produced fluorescence when incubated with human acute monocytic leukemia THP-1 cells used as a positive control (Fig. 1*D*). DiR treatment also produced fluorescence in the presence of MVs obtained from either HS or FBS (Fig. 1*D*), confirming that the isolated MVs were lipid-bound vesicles.

Biochemical Characterization of Serum-derived MVs—Next, we fractionated the MV preparations by sucrose gradient centrifugation and determined the biochemical composition of each 1-ml fraction. The concentration of phospholipids, cholesterol, triglycerides, and lipoproteins (*i.e.* LDL and HDL) in each fraction was determined using standardized biochemical assays. Our results showed that MV fractions contained relatively high concentrations of phospholipids, averaging from 30 to 93 μM for HS-derived vesicles (Fig. 2*A*) and from 4 to 15 μM for FBS-derived vesicles (Fig. 2*B*). Cholesterol was detected in low amounts in HS-derived MVs (Fig. 2*A*, *fractions 4–6*, peak at 2 μM), but none was found in FBS-MVs (Fig. 2*B*). Triglycerides, LDL, and HDL were not detected in the MV fractions tested (Fig. 2, *A* and *B*; data not shown), indicating that the isolated MV fractions did not contain lipoproteins.

We then performed Western blot analysis to examine the proteins associated with serum-derived MVs. We found that ALP, a glycosylated membrane-bound enzyme associated with biomineralization processes (52, 53), was associated with the phospholipid-rich MV fractions (Fig. 2, *C* and *D*). The molecular weight of the ALP found in HS-MVs (55 kDa) was smaller than the one found in FBS-MVs (72 kDa), possibly indicating the presence of different ALP isoenzymes in these samples. We also detected the presence of the exosome-associated proteins TNFR1 and CD63 in phospholipid-rich fractions (Fig. 2, *C* and *D*), whereas other exosome proteins like LAMP2 were not detected in our specimens (data not shown).

Albumin, fetuin-A, and apoA-I were also found in association with serum-derived MVs (Fig. 2, *C* and *D*). Although fetuin-A and apoA-I were associated with fractions of lighter densities compared with fractions containing exosome proteins, the three serum proteins overlapped to some extent with exosome-associated proteins. These serum proteins have been consistently associated with mineralo-organic NPs derived from body fluids, and they have been shown to act as both inhibitors and seeders of mineral particles in culture (9–11).

The structural and morphological data reported here along with the co-distribution of phospholipids and exosome proteins confirmed that the particles isolated from serum consisted of MVs and included exosomes. Given that the sizes of the isolated MVs (20–400 nm) exceeded the sizes reported previously for exosomes (30–100 nm) (32–34), we concluded that other vesicles, possibly microvesicles and apoptotic bodies, may also be present in our MV preparations.

Serum-derived MVs Induce Mineral Precipitation in Culture—To determine whether serum MVs may induce the formation of mineralo-organic NPs and mineral precipitation in body fluids,

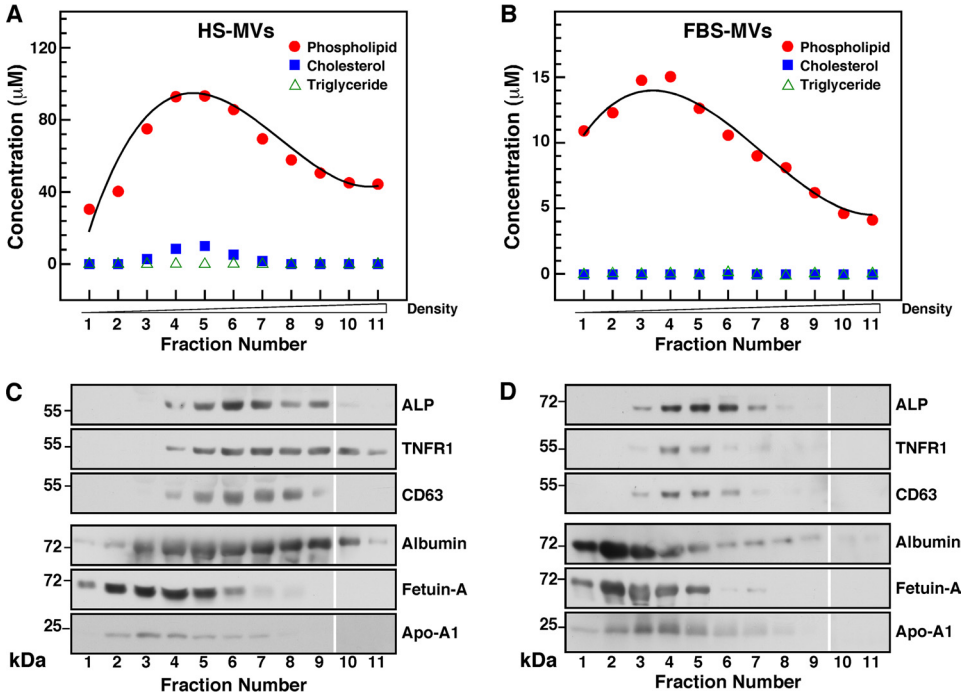

FIGURE 2. **Biochemical characterization of serum-derived MVs.** *A* and *B*, lipid characterization of serum MVs. MVs isolated by ultracentrifugation as in Fig. 1 were further fractionated by sucrose gradient centrifugation as described under "Materials and Methods." The phospholipid, cholesterol, and triglyceride content of each 1-ml fraction were assessed using standardized biochemical assays. *C* and *D*, protein characterization of serum MVs. Proteins from individual MV fraction corresponding to 60 μg of total proteins were separated by SDS-PAGE under denaturing and reducing conditions and analyzed by Western blotting with the indicated antibodies. The blots shown here were assembled from two different gels run in parallel, and they are separated by a *blank space* between fractions 9 and 10.

we inoculated MVs into DMEM and incubated the resulting mixture in cell culture conditions for several days (Fig. 3*A*). Although the addition of MVs into DMEM produced no turbidity following inoculation at day 0, precipitation visible to the naked eye was observed in most wells containing MVs after 1 week of incubation (Fig. 3*A*). The precipitation increased in a dose-dependent manner with the amount of MVs added and was more abundant for FBS-MVs than for HS-MVs. The level of visible precipitation continued to gradually increase with time, as seen after 2 weeks of incubation (Fig. 3*A*, *1 Week versus 2 Weeks*). The observations of visible MV-induced precipitation were consistent with the turbidity increase monitored by spectrophotometry at a wavelength of 650 nm (Fig. 3*A*, A_{650}). To confirm that serum MVs induce the formation of mineral precipitates in culture, we used another assay that monitors calcium deposition in a non-radioactive manner. We noticed that DMEM containing MVs showed a time-dependent increase in calcium deposition during incubation, whereas no calcification was observed in DMEM alone (Fig. 3*B*). As seen earlier (Fig. 3*A*), precipitation levels produced by FBS-MVs were slightly higher than those produced by HS-MVs (Fig. 3*B*).

To identify the biochemical component of MV fractions that induces mineral precipitation, we inoculated MV fractions obtained by sucrose gradient centrifugation into DMEM and measured the level of mineral precipitation following incubation in different cell culture conditions. After 2 months of incubation, the MV fractions containing high levels of phospholipids induced higher levels of mineral precipitation than MV fractions containing low amounts of phospholipids (Fig. 3*C*). Similar results were obtained for incubation periods of either 2 weeks or 1 month (data not shown). These results indicate that phospholipid-rich MV fractions induce mineral precipitation in culture.

In order to evaluate whether MVs induce mineral precipitation by binding to calcium and phosphate ions in cell culture medium, we inoculated MVs into DMEM and treated the resulting mixture with calcium and phosphate ions to induce mineral precipitation. We have shown previously (9–11) that the addition of calcium and phosphate ions in DMEM containing a body fluid produces mineral precipitates without the delay usually required for mineral NPs to spontaneously form in culture. Here, a constant amount of MVs was added into DMEM, followed by the addition of calcium and phosphate ions at 0.1–3 mM each. After overnight incubation in cell culture conditions, the precipitates were harvested by centrifugation and subjected to Western blot analysis to detect MV proteins (Fig. 3, *D* and *E*).

Whole HS used as a control showed the presence of the proteins ALP (low signal), TNFR1, and CD63 as well as albumin, fetuin-A, and apoA-I (Fig. 3*D*, *lane 1*). In the case of whole FBS, all of these proteins were detected (Fig. 3*E*, *lane 1*). As shown earlier in Fig. 2, *C* and *D*, HS-MVs and FBS-MVs harbored ALP, TNFR1, CD63, albumin, fetuin-A, and apoA-I (Fig. 3, *D* and *E*, *lane 2*). When MVs were added into DMEM and centrifuged at low speed (12,000 × *g*), the vesicles could not be pelleted, as seen by the absence of MV-associated proteins in this control experiment (Fig. 3, *D* and *E*, *lane 3*). However, after inoculation of MVs into DMEM and incubation for 1 day in cell culture conditions prior to low speed centrifugation, several MV proteins were detected (Fig. 3, *D* and *E*, *lane 4*), suggesting that MVs induced the formation of mineral precipitate following

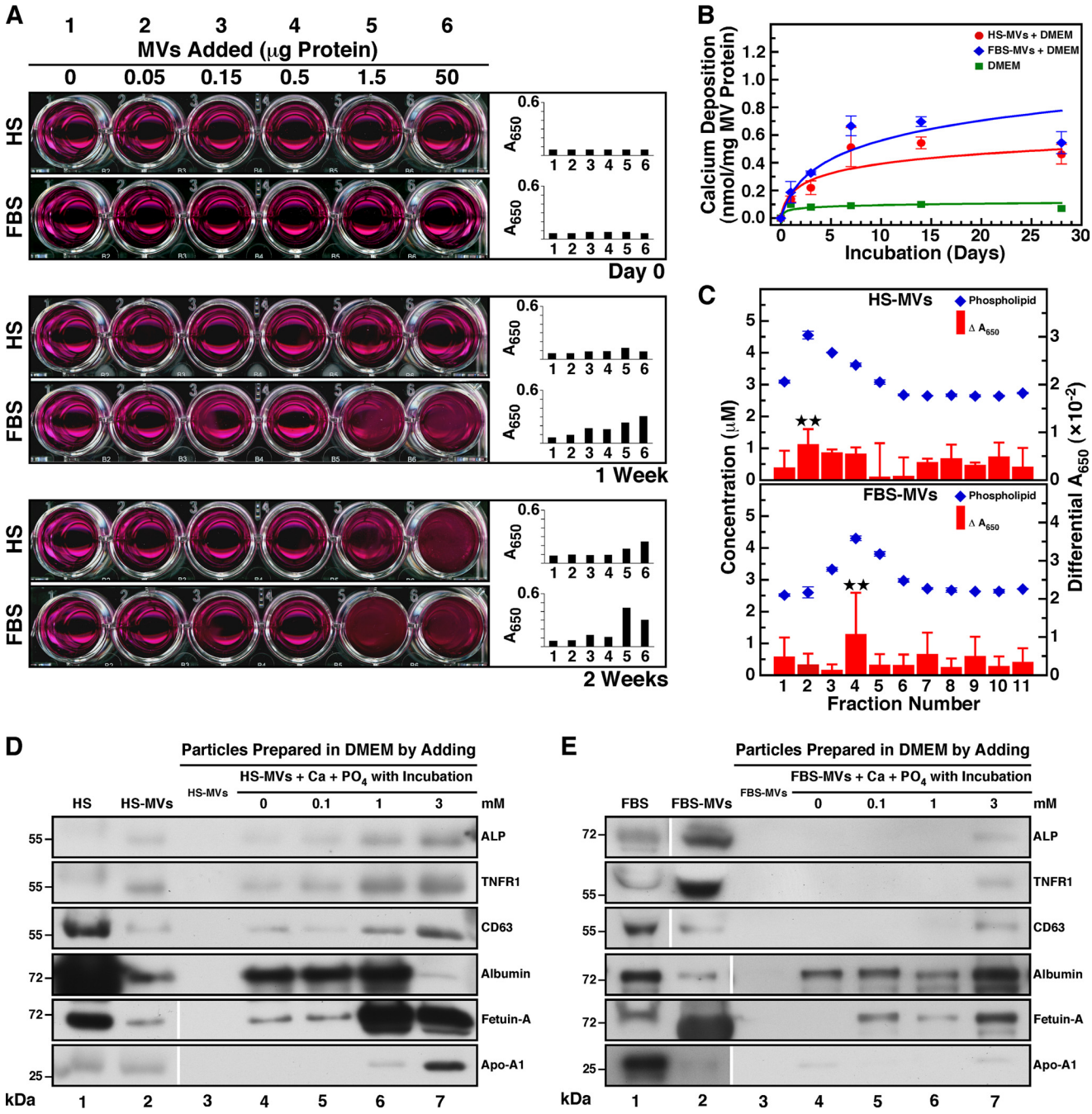

FIGURE 3. **Serum MVs induce mineral precipitation in cell culture conditions.** *A*, MVs prepared by ultracentrifugation from HS and FBS were quantified based on total protein content prior to inoculation into DMEM at the amount indicated (*Day 0*, final volume of 1 ml). The solutions were incubated in cell culture conditions for the time indicated. MVs produced visible precipitation that increased in a time-dependent manner. DMEM used as a negative control produced no precipitation. *B*, the ability of MVs isolated by sucrose gradient centrifugation to undergo calcification. Phospholipid-rich MV fractions corresponding to 30 μg of total protein were added into DMEM and incubated in cell culture conditions. Precipitates were collected at the time indicated following centrifugation at 12,000 $\times$ *g* for 30 min, and the calcium content was determined using the *O*-cresolphthalein complexone assay. Both HS-MVs and FBS-MVs induced the formation of calcified precipitate in a time-dependent manner during incubation. *C*, phospholipid-rich MV fractions induce mineral precipitation in culture. 100 μl of each sucrose gradient fraction was added into DMEM in a final volume of 1 ml prior to incubation in cell culture conditions for 2 months. Mineral precipitation was assessed by A_{650} turbidity readings. Turbidity observed before incubation was subtracted from the turbidity reading obtained after incubation (*Differential* A_{650}). The content of phospholipids was determined using a standardized biochemical assay. Phospholipid-rich fractions produced slightly higher levels of precipitation under these conditions. *D* and *E*, Western blotting analysis of co-precipitates containing MVs and mineralo-organic NPs. MVs were inoculated into DMEM, and $CaCl_2$ and NaH_2PO_4 were added at the concentration indicated in a final volume of 1 ml prior to incubation in cell culture conditions for 1 day. Mineral precipitates were pelleted by centrifugation at 12,000 $\times$ *g* for 30 min prior to washing steps in HEPES buffer. Equal amounts (60 μg) of proteins from whole serum, MVs, or MV-NP co-precipitates were separated under denaturing and reducing conditions by SDS-PAGE and probed with the indicated antibodies. Some of the *lanes* shown here originated from two different gels run in parallel; these are delineated by the *blank space* seen in some of the blots. **, $0.1 < p < 0.5$. *Error bars*, S.E.

incubation and that this precipitate was heavy enough to be pelleted by the low speed centrifugation used. When HS-MVs were incubated into DMEM with exogenous calcium and phosphate ions were added at 0.1–3 mM each, MV-associated proteins were also detected, and most proteins (ALP, TNFR1, CD63, and apoA-I) produced signals that increased in a dose-

dependent manner with the concentration of ions added (Fig. 3*D*, *lanes 5–7*), indicating that MVs interacted with the exogenous ions to produce a mineral precipitate. In the case of FBS-MVs, protein signals were also detected for all MV proteins (Fig. 3*E*, *lanes 5–7*; note that ALP, TNFR1, CD63, and apoA-I produced signals only after the addition of ions at 3 mM).

These results suggest that the isolated serum MVs induce the formation of calcium-containing precipitates in culture. These MVs may induce the formation of mineral precipitates by binding to exogenous calcium and phosphate ions in cell culture conditions.

Morphological and Mineral Characterization of Mineralo-organic NPs Seeded by MVs—To verify the nature of the precipitation induced by MVs, we submitted the precipitates (obtained in Fig. 3*A*) to TEM analysis without fixation or staining. The precipitates produced following inoculation of MVs into DMEM consisted of small, round, electron-dense particles of sizes varying from 10 to 400 nm (Fig. 4*A*). The fact that these particles could be observed without staining suggested that they may be coated with an electron-dense material like minerals (compare the negatively stained, non-mineralized MVs shown in Fig. 1*C* with the unstained, mineralized MV-seeded particles in Fig. 4*A*). Mineralization of the particles was confirmed by electron diffraction analysis, which showed several concentric rings corresponding to a polycrystalline mineral (Fig. 4*A*, *insets*). Particles of similar size, morphology, and electron density were noted in the precipitates seeded by FBS-MVs (Fig. 4*A*). We confirmed the presence of MV proteins in the seeded mineral NPs by Western blots (Fig. 4*A*, *right panels*). Overall, the particles seeded by MVs were similar to the particles described earlier as NB (6, 54). No mineral particles could be pelleted by centrifugation of incubated DMEM (data not shown), consistent with the observation that DMEM alone does not produce mineral NPs under these conditions (4, 5).

We also inoculated MVs into DMEM containing either 5% HS or FBS prior to incubation for 2 weeks to compare the nature of the particles obtained with and without serum. The mixtures of MVs, DMEM, and serum produced mineral NPs of a crystalline nature following incubation (Fig. 4*B*). Accordingly, the electron diffraction patterns of these particles (Fig. 4*B*, *insets*) showed concentric rings that were more pronounced than that of the particles seeded without serum (Fig. 4*A*, *insets*). The particles obtained this way appeared larger in size compared with the particles prepared without added serum (Fig. 4*B*, 20–500 nm). All of the proteins found earlier in MVs (Fig. 2, *C* and *D*) were detected within the MV-seeded mineral NPs (Fig. 4*B*, *right panels*).

Notably, the mineral particles seeded by MVs and serum were highly similar not only to NB (6, 54) but also to the secondary calciprotein particles (CPPs) observed by Jahnen-Dechent and colleagues in specimens obtained from patients undergoing dialysis (55) or suffering from calcifying peritonitis (27). These observations suggest that, in addition to MVs, serum may provide additional compounds that induce crystallization of the mineral particles following prolonged incubation.

Next, we used EDX and FTIR spectroscopies to identify the mineral phase associated with MV-seeded particles. Previous studies have shown that the so-called NB (5, 56) and the mineralo-organic NPs observed in calcified human tissues (30, 57) consist of carbonate HAP, a mineral similar to the one found in bones and teeth of vertebrates (58, 59). EDX spectra of mineral particles seeded by MVs in DMEM showed major peaks of carbon (*C*), calcium (*Ca*), oxygen (*O*), sodium (*Na*), phosphorus (*P*), and sulfur (*S*) (Fig. 4*C*, *HS-MVs+DMEM* and *FBS-MVs+DMEM*), consistent with the presence of carbonate-calcium phosphate in MV-seeded NPs. Similarly, the particles seeded by MVs in DMEM containing serum showed similar peaks consistent with the formation of carbonate-calcium phosphate (Fig. 4*C*, *HS-MVs+DMEM+HS* and *FBS-MVs+DMEM+FBS*).

FTIR analysis revealed major peaks of phosphate at 566 cm^{-1}, 604 cm^{-1}, 960 cm^{-1}, and 1,033–1,100 cm^{-1} in the particles seeded by MVs in DMEM with or without serum (Fig. 4*D*; compare with the spectra of commercial $Ca_3(PO_4)_2$ and HAP shown for reference; see also Refs. 60 and 61). In addition, peaks corresponding to carbonate at 875 and 1,430 cm^{-1} were found in MV-seeded particles (Fig. 4*D*; compare with the signals obtained for $CaCO_3$; see also Refs. 62 and 63). For comparison, a sample of mineralo-organic NPs prepared by adding calcium and phosphate into DMEM containing 5% FBS showed similar phosphate and carbonate peaks (Fig. 4*D*, *FBS-NPs*). These FTIR spectra were consistent with the presence of carbonate HAP within the MV-seeded particles. Other peaks corresponding to H_2O and the amide bonds of serum proteins were also detected in the seeded particles (Fig. 4*D*; see also Refs. 58, 64, and 65). These spectroscopy analyses confirm that the MV-seeded particles contain carbonate HAP similar to the particles described earlier as NB (7) and to the mineralo-organic NPs found in calcified human tissues (30).

PS on the Surface of MVs Contributes to Mineral NP Seeding—PS appears to represent a nucleator of calcium phosphate in matrix vesicles (38, 66). Several MV populations, such as those released by platelets and apoptotic cells, harbor PS on their surface (67, 68), but it is unclear whether PS acts as a nucleator in this context. We first used Western blot analysis to examine whether the PS-binding protein annexin V is present in serum MV fractions. Annexin V was not detected in either HS-MVs or FBS-MVs (Fig. 5*A*; a HeLa cell lysate was used as positive control). Next, we examined whether PS is present on MVs by using immunogold labeling and annexin V as a probe. TEM images showed that annexin V binds the surface of MVs isolated from HS or FBS (Fig. 5*B*). Similarly, using fluorescence spectroscopy, we observed that annexin V that was prelabeled with the fluorochrome FITC interacts with MVs of both human and bovine origins. As a control, the interaction between PS and annexin V, which requires free calcium (69), was abrogated by the addition of the calcium chelator EDTA (Fig. 5*C*). These results confirm that PS is present on the surface of MVs isolated from serum.

We investigated whether PS found on the surface of MVs contributes to the seeding of mineralo-organic NPs by the vesicles. We incubated MVs with an anti-PS antibody and measured the seeding potential of MVs following the washing steps. Blocking PS moieties with the antibody significantly decreased seeding of mineral NPs by MVs, whereas an anti-CD63 antibody used as a negative control showed no effect on seeding (Fig. 5*D*). These data indicate that PS contributes to the seeding activity of MVs.

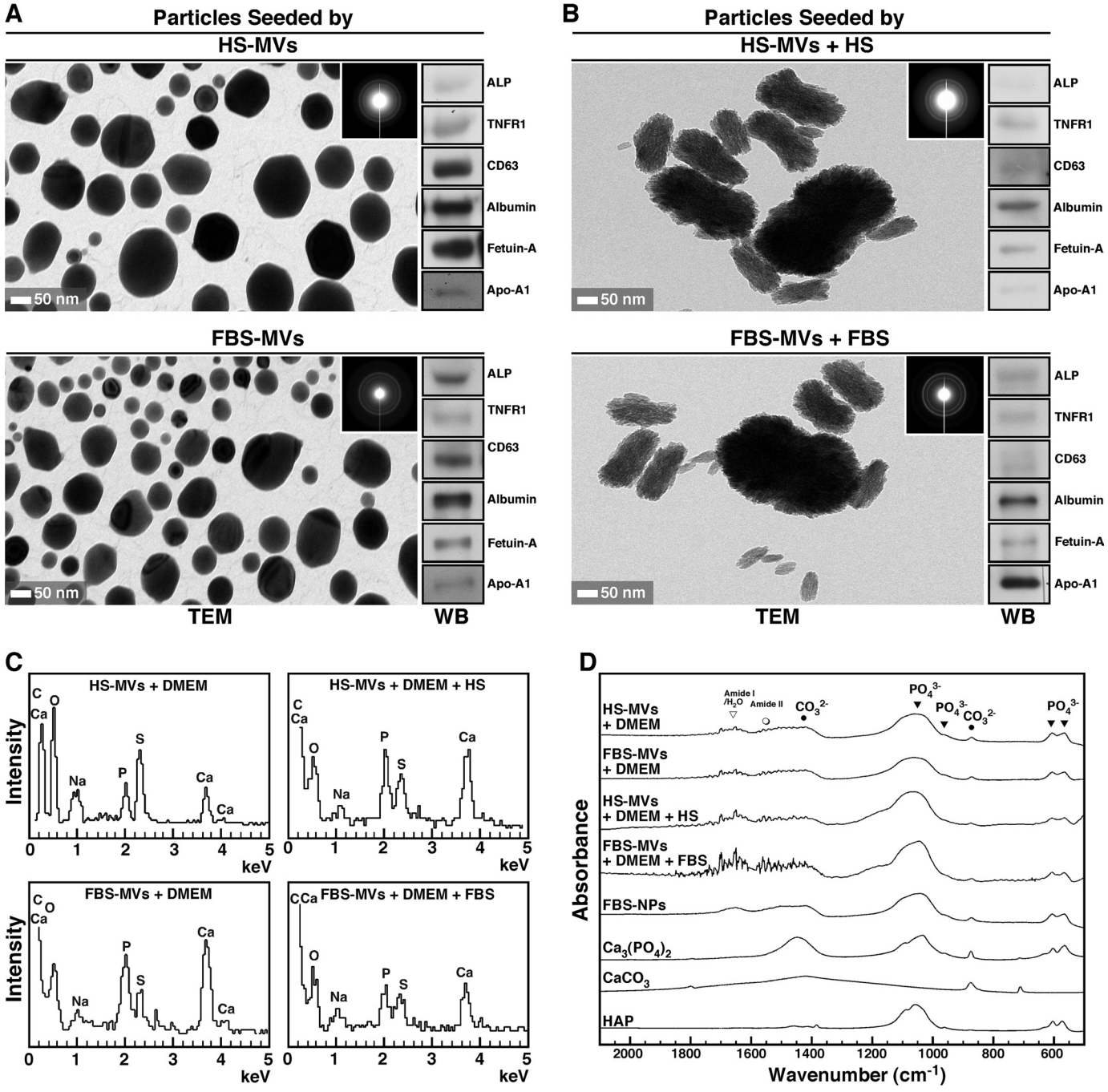

FIGURE 4. **MV-induced mineral precipitation represents calcium phosphate mineralo-organic NPs.** *A*, mineral precipitates obtained from DMEM containing MVs as in Fig. 3*A* were harvested by centrifugation and analyzed by TEM without fixation or staining. The precipitates displayed round NPs with a dark electron-dense structure. The polycrystalline, mineralized nature of the particles was confirmed by the concentric rings produced on electron diffraction patterns (*insets*). Western blotting analysis revealed the presence of MV-associated proteins within the seeded mineralo-organic NPs (*right panels*). *B*, mineral precipitates obtained from DMEM containing both MVs and 5% serum showed ellipsoid NPs of a polycrystalline nature (*insets*). MV-associated proteins were also detected in these particles (*right panels*). *C*, EDX spectra of mineral particles seeded by MVs with or without 5% serum showed peaks corresponding to carbon, calcium, oxygen, sodium, phosphorus, and sulfur. *D*, FTIR analysis revealed the presence of both phosphate groups at 566, 604, and 960 cm^{-1} and between 1,033 and 1,100 cm^{-1} and carbonate at 875 and 1,430 cm^{-1}, consistent with the presence of carbonate apatite. Peaks corresponding to water and the amide bonds of proteins were also observed in MV-seeded particles. Mineralo-organic NPs prepared by adding 1 mM $CaCl_2$ and NaH_2PO_4 each in 1 ml of DMEM containing 5% FBS showed similar peaks (*FBS-NPs*). Commercial powders of $Ca_3(PO_4)_2$, $CaCO_3$, and HAP were included for comparison. *WB*, Western blot.

DISCUSSION

In the present study, we show that serum MVs isolated by ultracentrifugation and sucrose gradient centrifugation induce the formation of mineral NPs similar to the so-called NB following incubation in cell culture conditions. These results indicate that MVs may represent the long sought nucleator of mineralo-organic NPs in body fluids. Moreover, these observations support our previous studies showing that NB-like structures represent non-living mineral NPs that possess biomimetic properties (9, 16).

The MVs isolated from serum harbor various proteins, including ALP, exosome markers (TNFR1 and CD63), and

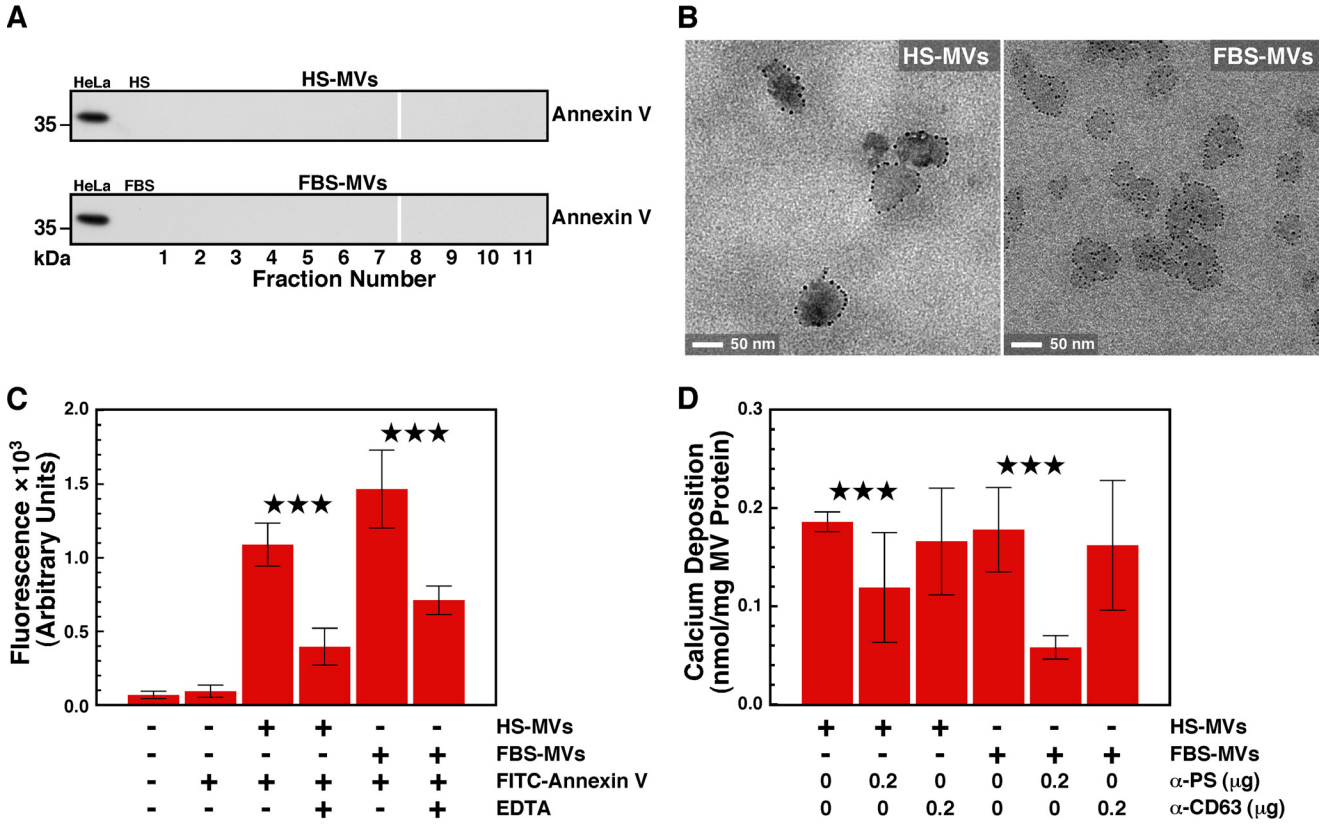

FIGURE 5. **PS exposed on the surface of serum MVs contributes to seeding of mineralo-organic NPs.** *A*, Western blotting showing the absence of annexin V on MVs isolated from either HS or FBS by sucrose gradient centrifugation. Equal amounts of proteins (60 μg) from either HeLa cell lysates (positive control), whole serum, or MV fractions (corresponding to the same fractions as in Fig. 2) were separated under denaturing and reducing conditions on SDS-PAGE and probed with anti-annexin V antibody. *B*, annexin V-immunogold labeling of serum MVs. Fixed and stained thin sections of MVs were treated sequentially with annexin V, rabbit anti-annexin V antibody, and gold-conjugated anti-rabbit antibody prior to observation by TEM. Binding of the gold particles to MVs revealed the presence of PS on the vesicles' surface. *C*, annexin V-fluorescence labeling of serum MVs. MVs corresponding to 30 μg of total protein content were incubated for 30 min at room temperature with FITC-labeled annexin V in 100 μl of HEPES buffer prior to centrifugation and washing steps. Both HS-MVs and FBS-MVs produced fluorescence, which was abrogated by the calcium chelator EDTA (0.5 mM). Reaction mixtures containing either no reagents or FITC-annexin V alone were processed as above and used as negative controls. *D*, PS contributes to MV-induced mineral seeding. MVs (2 mg of total proteins) were treated with either anti-PS or anti-CD63 antibody (0.2 μg/ml) for 1 h at room temperature. MVs were then pelleted, washed, and incubated in DMEM for 1 week before measuring calcium deposition. ***, $p < 0.01$. *Error bars*, S.E.

serum proteins (albumin, fetuin-A, and apoA-I; Fig. 6*A*). The size of the isolated MVs (30–180 nm) and the presence of exosome markers indicate that exosomes represent the major vesicles present in our preparations, consistent with previous results obtained with a similar fractionation protocol (32). Given that the sizes of the MVs isolated here (30–180 nm) are slightly larger than the sizes reported previously for exosomes (30–100 nm), it is possible that microvesicles and apoptotic bodies may represent minor constituents of our MV specimens. The minor differences in the composition of the MVs isolated here and in previous studies may be due to the nature of the starting material (*e.g.* serum *versus* plasma) as well as variation in sample preparation (70), among others.

ALP, a phosphatase enzyme found on the surface of matrix vesicles (34, 53, 71), is found in association with the serum MVs described here. Hunter *et al.* (72) have observed that blocking ALP activity with specific inhibitors considerably decreases the formation of mineral particles from tissue homogenate culture. These observations support the possibility that ALP may contribute to the seeding of mineralo-organic NPs in this context.

In the case of serum proteins, we proposed in a previous study (11) that albumin and fetuin-A may initially inhibit mineral particle formation but may eventually nucleate particle formation and deposition once the concentrations of calcium and phosphate exceed saturation levels. The results obtained in the present study appear to support this proposal, because albumin and fetuin-A were found in association with MVs, which in turn induced the formation of mineralo-organic NPs in culture.

The presence of PS on the surface of MVs suggests a possible mechanism to account for the formation of mineralo-organic NPs induced by serum MVs (Fig. 6*B*). PS possesses calcium-binding properties (38–40), and its presence on the surface of MVs suggests that this phospholipid may serve as a binding site for calcium and phosphate ions. Binding of calcium and phosphate on the surface of MVs may induce mineral precipitation and lead to the formation of fully crystallized mineral particles with time. Such mineral NPs have been shown to evolve into mineralized biofilm-like structures, as seen previously for the so-called NB (5) and mineralo-organic NPs (9). Notably, several human diseases, including include cancer, diabetes, malaria, sickle cell anemia, thalassemia, and uremia, have been associated with increased exposure of PS on MVs or cells (73), suggesting that PS may also contribute to mineral NP formation in these conditions.

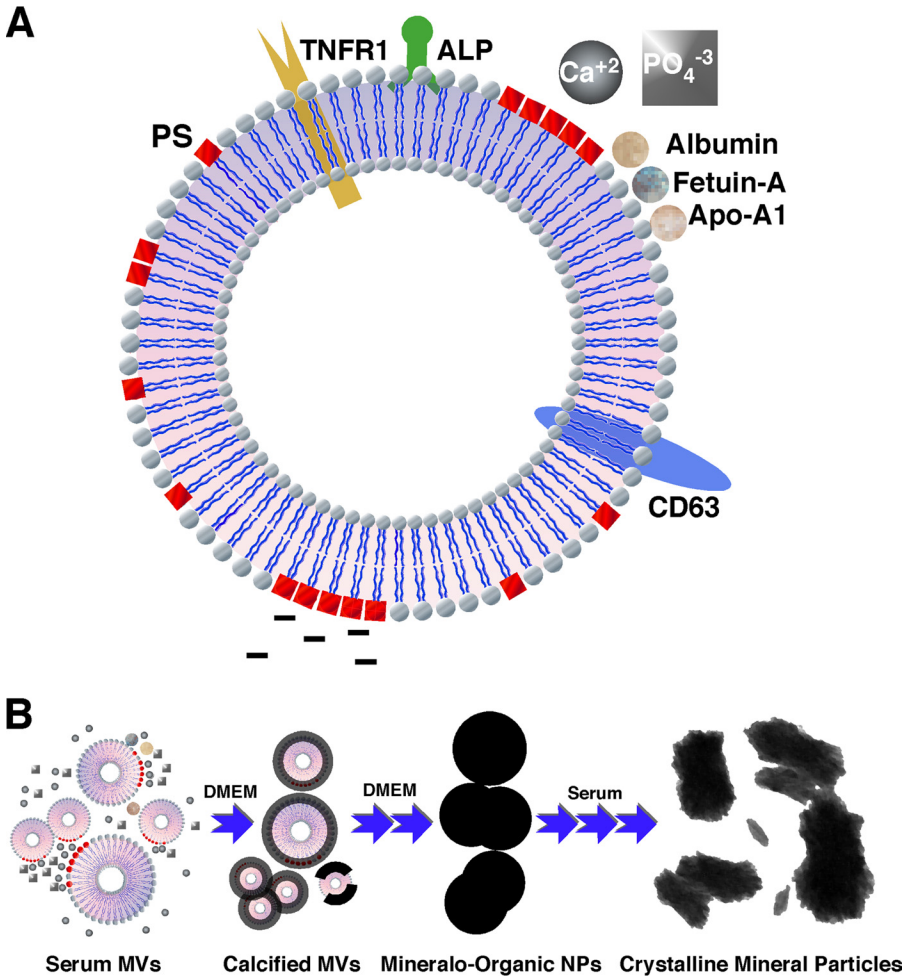

FIGURE 6. **Schematic model illustrating the composition of MVs and the seeding of mineralo-organic NPs by MVs.** *A*, illustration representing an MV isolated from serum in the present study. Our results indicate that the isolated MVs consist of phospholipid-bound vesicles containing ALP, TNFR1, CD63, albumin, fetuin-A, and apoA-I. PS was found in the outer phospholipid layer of MVs. *B*, calcium ions present in cell culture medium and body fluids may bind to PS exposed on the surface of MVs and induce mineral precipitation. With time, mineralization of MVs may further increase and lead to the formation of fully mineralized mineralo-organic NPs similar to the so-called NB. Molecules present in serum and body fluids may promote the crystallization of the mineral particles and produce mineral precipitates similar to those observed previously in human calcified tissues.

We observed that FBS-MVs possess a higher mineral seeding ability compared with HS-MVs (Fig. 3, *A* and *B*). Fetal serum (*i.e.* FBS) may represent a better pro-calcifying milieu needed for bone and teeth formation compared with adult serum (HS). If this is the case, FBS-MVs may show functional differences compared with HS-MVs; accordingly, ALP appears to be present in slightly higher amounts in FBS-MVs compared with HS-MVs (Figs. 2 (*C* and *D*) and 4 (*A* and *B*)), an observation that may partially explain the difference in seeding ability of these vesicles.

Our results may have important implications for the understanding of ectopic calcification in humans. For one, MVs may induce the formation of mineral NPs in tissues and body fluids under certain conditions. Although the exact nature of these circumstances has not been examined in the present study, various conditions could possibly induce MV-mediated seeding of mineral NPs *in vivo*. For instance, a decrease in the level of calcification inhibition proteins, an increase of calcium and phosphate concentrations due to kidney failure, a disturbance of vitamin D physiological activity, or an increase in the production of MVs due to inflammation or hyperlipidemia may lead to MV-induced formation of mineral NPs. In addition, given that MVs are present in most body fluids, it appears plausible that these entities may induce the formation of mineralo-organic NPs in other areas of the body. Further studies are currently under way to assess the relevance of MV-induced ectopic calcification *in vivo*.

A prominent factor that may induce the formation of MVs and ectopic calcification *in vivo* is inflammation (40). Chronic inflammation can induce the differentiation of VSMCs into osteoblast-like cells that produce matrix vesicles, which in turn induce ectopic calcification. A recent study by Aikawa *et al.* (74) has shown that inflammation precedes ectopic calcification in a mouse apolipoprotein E-deficient model of atherosclerosis, suggesting that inflammation may lead to ectopic calcification. These authors concluded that macrophages infiltrating the sites of lipid accumulation secrete cytokines that induce the phenotypic differentiation of VSMCs into functional osteoblast-like cells. Given that calcium phosphate displays pro-inflammatory properties (75–77), Shanahan (78) suggested that these processes may lead to a vicious cycle of inflammation and calcification, which would eventually propitiate atherosclero-

sis. We recently found that mineralo-organic NPs of calcium phosphate do not activate pro-inflammatory reactions in macrophages but that large particle aggregates led to caspase-1 activation and secretion of pro-inflammatory IL-1β (17). These results suggest that mineral NPs nucleated by MVs may initially be inert in the body but may eventually induce inflammation and participate in disease processes after reaching a certain size.

Apoptosis represents another factor that may control the formation of mineral NPs and ectopic calcification in the body. A previous study by Proudfoot *et al.* (44) showed that VSMCs calcify after about 28 days in culture and that apoptosis appears prior to mineral precipitation. Blocking apoptosis with a pan-caspase inhibitor reduced calcification, whereas induction of apoptosis with anti-Fas IgM increased calcification in culture. In the end, calcification was attributed to the release of apoptotic bodies (44) similar to the MVs studied here.

Obviously, differences may exist between the *in vitro* system studied here and what might occur in the human body. For instance, the observation that PS is exposed on the surface of MVs suggests that these MVs could be subject to constant phagocytosis and clearance by macrophages of the reticuloendothelial system *in vivo*. It remains to be seen under what conditions procalcifying MVs similar to the ones characterized here may accumulate at amounts high enough in body fluids to induce the formation of mineralo-organic NPs and larger calcified deposits.

Jahnen-Dechent and colleagues (79, 80) have proposed that mineral NPs in the form of CPPs may be part of a larger physiological cycle that controls the use and clearance of mineral ions in the body. These authors have proposed that serum proteins like fetuin-A may serve as systemic calcification inhibitors and chaperone molecules that stabilize excess calcium and phosphate in the form of CPPs, leading to clearance of the particles by the reticuloendothelial system (81). Recently, these authors have shown that the scavenger receptor-A present on macrophages is implicated in the recognition and rapid clearance of CPPs from the blood of mice (82).

From another perspective, we noticed that the MVs isolated from serum (Fig. 1, *A* and *B*) share similarities with a group of intriguing particles described previously in the blood under various names, including "microzymas," "protits," "somatids," "cancer bacteria," "pleomorphic bacteria," and "filterable bodies," among other terms (83–86). Vodyanoy and colleagues (87) have reported that metal nanoclusters may form structures referred to as "proteons" when they bind to denatured proteins in various body fluids, such as blood. Based on these and similar observations (8–17), we believe that the putative microzymas, protits, somatids, and related entities may represent a combination of various particles that form spontaneously in the blood during incubation, which may include MVs, mineralo-organic NPs, proteons, and cellular remnants. Further studies are needed to verify this intriguing possibility.

In summary, our results indicate that human and bovine sera contain MVs that are able to induce the formation of mineralo-organic NPs when incubated in cell culture medium. These results suggest that the formation of mineral NPs and ectopic calcification occurring in the human body may be induced by MVs similar to the ones described here.

Acknowledgments—We thank Dr. Ching-Shiun Chen at Chang Gung University for help with FTIR; Dr. Po-Wen Gu for help with lipid analysis; and Hwei-Chung Liu, Ji-Lung Peng, Hsi-Chien Su, Hui-Chun Kung, and Ya-Ling Chen for expertise in microscopy.

Note Added in Proof—We have recently extended the findings on calcium apatite nanoparticles to other types of cations which also assemble nano- and micro-scale structures resembling biological topologies, which we have termed collectively as *bions* (Wu, C. Y., Young, L., Young, D., Martel, J., Young, J. D. (2013) *Bions*: A family of biomimetic mineralo-organic complexes derived from biological fluids. *PLoS One* **8,** e75501).

REFERENCES

1. Donaldson, K., Murphy, F. A., Duffin, R., and Poland, C. A. (2010) Asbestos, carbon nanotubes and the pleural mesothelium. A review of the hypothesis regarding the role of long fibre retention in the parietal pleura, inflammation and mesothelioma. *Part. Fibre Toxicol.* **7,** 5
2. Chen, J., Dong, X., Zhao, J., and Tang, G. (2009) *In vivo* acute toxicity of titanium dioxide nanoparticles to mice after intraperitioneal injection. *J. Appl. Toxicol.* **29,** 330–337
3. Kim, B. Y., Rutka, J. T., and Chan, W. C. (2010) Nanomedicine. *N. Engl. J. Med.* **363,** 2434–2443
4. Kajander, E. O., Kuronen, I., Akerman, K., Peltarri, A., and Cifcioglu, N. (1997) Nanobacteria from blood, the smallest culturable autonomously replicating agent on Earth. *Proc. Soc. Photo-Opt. Intrum. Eng.* **3111,** 420–428
5. Kajander, E. O., and Ciftçioglu, N. (1998) Nanobacteria. An alternative mechanism for pathogenic intra- and extracellular calcification and stone formation. *Proc. Natl. Acad. Sci. U.S.A.* **95,** 8274–8279
6. Kajander, E. O., Ciftcioglu, N., Aho, K., and Garcia-Cuerpo, E. (2003) Characteristics of nanobacteria and their possible role in stone formation. *Urol. Res.* **31,** 47–54
7. Ciftcioglu, N., McKay, D. S., Mathew, G., and Kajander, E. O. (2006) Nanobacteria. Fact or fiction? Characteristics, detection, and medical importance of novel self-replicating, calcifying nanoparticles. *J. Investig. Med.* **54,** 385–394
8. Martel, J., and Young, J. D. (2008) Purported nanobacteria in human blood as calcium carbonate nanoparticles. *Proc. Natl. Acad. Sci. U.S.A.* **105,** 5549–5554
9. Young, J. D., Martel, J., Young, L., Wu, C. Y., Young, A., and Young, D. (2009) Putative nanobacteria represent physiological remnants and culture by-products of normal calcium homeostasis. *PLoS One* **4,** e4417
10. Young, J. D., Martel, J., Young, D., Young, A., Hung, C. M., Young, L., Chao, Y. J., Young, J., and Wu, C. Y. (2009) Characterization of granulations of calcium and apatite in serum as pleomorphic mineralo-protein complexes and as precursors of putative nanobacteria. *PLoS One* **4,** e5421
11. Wu, C. Y., Martel, J., Young, D., and Young, J. D. (2009) Fetuin-A/albumin-mineral complexes resembling serum calcium granules and putative nanobacteria. Demonstration of a dual inhibition-seeding concept. *PLoS One* **4,** e8058
12. Young, J. D., and Martel, J. (2010) The rise and fall of nanobacteria. *Sci. Am.* **302,** 52–59
13. Martel, J., Wu, C. Y., and Young, J. D. (2010) Critical evaluation of γ-irradiated serum used as feeder in the culture and demonstration of putative nanobacteria and calcifying nanoparticles. *PLoS One* **5,** e10343
14. Martel, J., Young, D., Young, A., Wu, C. Y., Chen, C. D., Yu, J. S., and Young, J. D. (2011) Comprehensive proteomic analysis of mineral nanoparticles derived from human body fluids and analyzed by liquid chromatography-tandem mass spectrometry. *Anal. Biochem.* **418,** 111–125
15. Peng, H. H., Martel, J., Lee, Y. H., Ojcius, D. M., and Young, J. D. (2011) Serum-derived nanoparticles. *De novo* generation and growth *in vitro*, and internalization by mammalian cells in culture. *Nanomedicine* **6,** 643–658
16. Martel, J., Young, D., Peng, H. H., Wu, C. Y., and Young, J. D. (2012) Biomimetic properties of minerals and the search for life in the Martian

meteorite ALH84001. *Annu. Rev. Earth Planet. Sci.* **40,** 167–193
17. Peng, H. H., Wu, C. Y., Young, D., Martel, J., Young, A., Ojcius, D. M., Lee, Y. H., and Young, J. D. (2013) Physicochemical and biological properties of biomimetic mineralo-protein nanoparticles formed spontaneously in biological fluids. *Small* **9,** 2297–2307
18. Cisar, J. O., Xu, D. Q., Thompson, J., Swaim, W., Hu, L., and Kopecko, D. J. (2000) An alternative interpretation of nanobacteria-induced biomineralization. *Proc. Natl. Acad. Sci. U.S.A.* **97,** 11511–11515
19. Vali, H., McKee, M. D., Ciftcioglu, N., Sears, S. K., Plows, F. L., Chevet, E., Ghiabi, P., Plavsic, M., Kajander, E. O., and Zare, R. N. (2001) Nanoforms: A new type of protein-associated mineralization. *Geochim. Cosmochim. Acta* **65,** 63–74
20. Drancourt, M., Jacomo, V., Lépidi, H., Lechevallier, E., Grisoni, V., Coulange, C., Ragni, E., Alasia, C., Dussol, B., Berland, Y., and Raoult, D. (2003) Attempted isolation of *Nanobacterium* sp. microorganisms from upper urinary tract stones. *J. Clin. Microbiol.* **41,** 368–372
21. Barr, S. C., Linke, R. A., Janssen, D., Guard, C. L., Smith, M. C., Daugherty, C. S., and Scarlett, J. M. (2003) Detection of biofilm formation and nanobacteria under long-term cell culture conditions in serum samples of cattle, goats, cats, and dogs. *Am. J. Vet. Res.* **64,** 176–182
22. Raoult, D., Drancourt, M., Azza, S., Nappez, C., Guieu, R., Rolain, J. M., Fourquet, P., Campagna, B., La Scola, B., Mege, J. L., Mansuelle, P., Lechevalier, E., Berland, Y., Gorvel, J. P., and Renesto, P. (2008) Nanobacteria are mineralo fetuin complexes. *PLoS Pathog.* **4,** e41
23. Höhling, H. J., Arnold, S., Plate, U., Stratmann, U., and Wiesmann, H. P. (1997) Analysis of a general principle of crystal nucleation, formation in the different hard tissues. *Adv. Dent. Res.* **11,** 462–466
24. Robinson, C., Connell, S., Kirkham, J., Shore, R., and Smith, A. (2004) Dental enamel—A biological ceramic: Regular substructures in enamel hydroxyapatite crystals revealed by atomic force microscopy. *J. Mater. Chem.* **14,** 2242–2248
25. Mahamid, J., Aichmayer, B., Shimoni, E., Ziblat, R., Li, C., Siegel, S., Paris, O., Fratzl, P., Weiner, S., and Addadi, L. (2010) Mapping amorphous calcium phosphate transformation into crystalline mineral from the cell to the bone in zebrafish fin rays. *Proc. Natl. Acad. Sci. U.S.A.* **107,** 6316–6321
26. Price, P. A., Thomas, G. R., Pardini, A. W., Figueira, W. F., Caputo, J. M., and Williamson, M. K. (2002) Discovery of a high molecular weight complex of calcium, phosphate, fetuin, and matrix γ-carboxyglutamic acid protein in the serum of etidronate-treated rats. *J. Biol. Chem.* **277,** 3926–3934
27. Heiss, A., Eckert, T., Aretz, A., Richtering, W., van Dorp, W., Schäfer, C., and Jahnen-Dechent, W. (2008) Hierarchical role of fetuin-A and acidic serum proteins in the formation and stabilization of calcium phosphate particles. *J. Biol. Chem.* **283,** 14815–14825
28. Matsui, I., Hamano, T., Mikami, S., Fujii, N., Takabatake, Y., Nagasawa, Y., Kawada, N., Ito, T., Rakugi, H., Imai, E., and Isaka, Y. (2009) Fully phosphorylated fetuin-A forms a mineral complex in the serum of rats with adenine-induced renal failure. *Kidney Int.* **75,** 915–928
29. Evan, A. P. (2010) Physiopathology and etiology of stone formation in the kidney and the urinary tract. *Pediatr. Nephrol.* **25,** 831–841
30. Schlieper, G., Aretz, A., Verberckmoes, S. C., Krüger, T., Behets, G. J., Ghadimi, R., Weirich, T. E., Rohrmann, D., Langer, S., Tordoir, J. H., Amann, K., Westenfeld, R., Brandenburg, V. M., D'Haese, P. C., Mayer, J., Ketteler, M., McKee, M. D., and Floege, J. (2010) Ultrastructural analysis of vascular calcifications in uremia. *J. Am. Soc. Nephrol.* **21,** 689–696
31. Hugel, B., Martínez, M. C., Kunzelmann, C., and Freyssinet, J. M. (2005) Membrane microparticles. Two sides of the coin. *Physiology* **20,** 22–27
32. György, B., Szabó, T. G., Pásztói, M., Pál, Z., Misják, P., Aradi, B., László, V., Pállinger, E., Pap, E., Kittel, A., Nagy, G., Falus, A., and Buzás, E. I. (2011) Membrane vesicles, current state-of-the-art. Emerging role of extracellular vesicles. *Cell. Mol. Life Sci.* **68,** 2667–2688
33. Keller, S., Sanderson, M. P., Stoeck, A., and Altevogt, P. (2006) Exosomes. From biogenesis and secretion to biological function. *Immunol. Lett.* **107,** 102–108
34. Théry, C., Ostrowski, M., and Segura, E. (2009) Membrane vesicles as conveyors of immune responses. *Nat. Rev. Immunol.* **9,** 581–593
35. Nieuwland, R., and Sturk, A. (2010) Why do cells release vesicles? *Thromb. Res.* **125,** S49–S51
36. Anderson, H. C., Mulhall, D., and Garimella, R. (2010) Role of extracellular membrane vesicles in the pathogenesis of various diseases, including cancer, renal diseases, atherosclerosis, and arthritis. *Lab. Invest.* **90,** 1549–1557
37. Daniel, L., Dou, L., Berland, Y., Lesavre, P., Mecarelli-Halbwachs, L., and Dignat-George, F. (2008) Circulating microparticles in renal diseases. *Nephrol. Dial. Transplant.* **23,** 2129–2132
38. Anderson, H. C., Garimella, R., and Tague, S. E. (2005) The role of matrix vesicles in growth plate development and biomineralization. *Front. Biosci.* **10,** 822–837
39. Golub, E. E. (2009) Role of matrix vesicles in biomineralization. *Biochim. Biophys. Acta* **1790,** 1592–1598
40. Golub, E. E. (2011) Biomineralization and matrix vesicles in biology and pathology. *Semin. Immunopathol.* **33,** 409–417
41. Bonucci, E. (2002) Crystal ghosts and biological mineralization. Fancy spectres in an old castle, or neglected structures worthy of belief? *J. Bone Miner. Metab.* **20,** 249–265
42. Leventis, P. A., and Grinstein, S. (2010) The distribution and function of phosphatidylserine in cellular membranes. *Annu. Rev. Biophys.* **39,** 407–427
43. Nomura, S., Ozaki, Y., and Ikeda, Y. (2008) Function and role of microparticles in various clinical settings. *Thromb. Res.* **123,** 8–23
44. Proudfoot, D., Skepper, J. N., Hegyi, L., Bennett, M. R., Shanahan, C. M., and Weissberg, P. L. (2000) Apoptosis regulates human vascular calcification *in vitro*. Evidence for initiation of vascular calcification by apoptotic bodies. *Circ. Res.* **87,** 1055–1062
45. Schinke, T., Amendt, C., Trindl, A., Pöschke, O., Müller-Esterl, W., and Jahnen-Dechent, W. (1996) The serum protein α2-HS glycoprotein/fetuin inhibits apatite formation *in vitro* and in mineralizing calvaria cells. A possible role in mineralization and calcium homeostasis. *J. Biol. Chem.* **271,** 20789–20796
46. Schafer, C., Heiss, A., Schwarz, A., Westenfeld, R., Ketteler, M., Floege, J., Muller-Esterl, W., Schinke, T., and Jahnen-Dechent, W. (2003) The serum protein α 2-Heremans-Schmid glycoprotein/fetuin-A is a systemically acting inhibitor of ectopic calcification. *J. Clin. Invest.* **112,** 357–366
47. Caby, M. P., Lankar, D., Vincendeau-Scherrer, C., Raposo, G., and Bonnerot, C. (2005) Exosomal-like vesicles are present in human blood plasma. *Int. Immunol.* **17,** 879–887
48. György, B., Módos, K., Pállinger, E., Pálóczi, K., Pásztói, M., Misják, P., Deli, M. A., Sipos, A., Szalai, A., Voszka, I., Polgár, A., Tóth, K., Csete, M., Nagy, G., Gay, S., Falus, A., Kittel, A., and Buzás, E. I. (2011) Detection and isolation of cell-derived microparticles are compromised by protein complexes resulting from shared biophysical parameters. *Blood* **117,** e39–e48
49. Garimella, R., Sipe, J. B., and Anderson, H. C. (2004) A simple and non-radioactive technique to study the effect of monophosphoesters on matrix vesicle-mediated calcification. *Biol. Proced. Online* **6,** 263–267
50. Lässer, C., Eldh, M., and Lötvall, J. (2012) Isolation and characterization of RNA-containing exosomes. *J. Vis. Exp.* **59,** e3037
51. Girotti, A. W., and Thomas, J. P. (1984) Superoxide and hydrogen peroxide-dependent lipid peroxidation in intact and triton-dispersed erythrocyte membranes. *Biochem. Biophys. Res. Commun.* **118,** 474–480
52. Whyte, M. P. (1994) Hypophosphatasia and the role of alkaline phosphatase in skeletal mineralization. *Endocr. Rev.* **15,** 439–461
53. Golub, E. E., and Boesze-Battaglia, K. (2007) The role of alkaline phosphatase in mineralization. *Curr. Opin. Orthop.* **18,** 444–448
54. Kajander, E. O., and Ciftcioglu, N. (1999) Nanobacteria as extremophiles. *Proc. Soc. Photo-Opt. Intrum. Eng.* **3755,** 106–112
55. Heiss, A., Jahnen-Dechent, W., Endo, H., and Schwahn, D. (2007) Structural dynamics of a colloidal protein-mineral complex bestowing on calcium phosphate a high solubility in biological fluids. *Biointerphases* **2,** 16–20
56. Kajander, E. O., Ciftcioglu, N., Miller-Hjelle, M. A., and Hjelle, J. T. (2001) Nanobacteria. Controversial pathogens in nephrolithiasis and polycystic kidney disease. *Curr. Opin. Nephrol. Hypertens.* **10,** 445–452
57. Evan, A. P., Coe, F. L., Rittling, S. R., Bledsoe, S. M., Shao, Y., Lingeman, J. E., and Worcester, E. M. (2005) Apatite plaque particles in inner medulla of kidneys of calcium oxalate stone formers. Osteopontin localization. *Kidney Int.* **68,** 145–154

58. Carden, A., and Morris, M. D. (2000) Application of vibrational spectroscopy to the study of mineralized tissues (review). *J. Biomed. Opt.* **5,** 259–268
59. Barrère, F., van Blitterswijk, C. A., and de Groot, K. (2006) Bone regeneration. Molecular and cellular interactions with calcium phosphate ceramics. *Int. J. Nanomedicine* **1,** 317–332
60. Barralet, J., Best, S., and Bonfield, W. (1998) Carbonate substitution in precipitated hydroxyapatite. An investigation into the effects of reaction temperature and bicarbonate ion concentration. *J. Biomed. Mater. Res.* **41,** 79–86
61. Vallet-Regi, M., and Ramila, A. (2000) New bioactive glass and changes in porosity during the growth of a carbonate hydroxyapatite layer on glass surfaces. *Chem. Mater.* **12,** 961–965
62. Aizenberg, J., Addadi, L., Weiner, S., and Lambert, G. (1996) Stabilization of amorphous calcium carbonate by specialized macromolecules in biological and synthetic precipitates. *Adv. Mater.* **8,** 222–226
63. Raz, S., Testeniere, O., Hecker, A., Weiner, S., and Luquet, G. (2002) Stable amorphous calcium carbonate is the main component of the calcium storage structures of the crustacean *Orchestia cavimana*. *Biol. Bull.* **203,** 269–274
64. Ayman, A., Talaat, M. S., Negm, S., and Talaat, H. (2008) Investigation of biophysical characteristics of diabetic living eye tissues using PA-FTIR-spectroscopy. *Eur. Phys. J. Spec. Top.* **153,** 497–501
65. Chen, C. W., Oakes, C. S., Byrappa, K., Riman, R. E., Brown, K., TenHuisen, K. S., and Janas, V. F. (2004) Synthesis, characterization, and dispersion properties of hydroxyapatite prepared by mechanochemical-hydrothermal methods. *J. Mater. Chem.* **14,** 2425–2432
66. Merolli, A., and Santin, M. (2009) Role of phosphatidyl-serine in bone repair and its technological exploitation. *Molecules* **14,** 5367–5381
67. Fadok, V. A., Bratton, D. L., Frasch, S. C., Warner, M. L., and Henson, P. M. (1998) The role of phosphatidylserine in recognition of apoptotic cells by phagocytes. *Cell Death Differ.* **5,** 551–562
68. Lentz, B. R. (2003) Exposure of platelet membrane phosphatidylserine regulates blood coagulation. *Prog. Lipid. Res.* **42,** 423–438
69. Huber, R., Schneider, M., Mayr, I., Römisch, J., and Paques, E. P. (1990) The calcium binding sites in human annexin V by crystal structure analysis at 2.0 Å resolution. Implications for membrane binding and calcium channel activity. *FEBS Lett.* **275,** 15–21
70. Yuana, Y., Bertina, R. M., and Osanto, S. (2011) Pre-analytical and analytical issues in the analysis of blood microparticles. *Thromb. Haemost.* **105,** 396–408
71. Théry, C., Zitvogel, L., and Amigorena, S. (2002) Exosomes. Composition, biogenesis and function. *Nat. Rev. Immunol.* **2,** 569–579
72. Hunter, L. W., Shiekh, F. A., Pisimisis, G. T., Kim, S. H., Edeh, S. N., Miller, V. M., and Lieske, J. C. (2011) Key role of alkaline phosphatase in the development of human-derived nanoparticles *in vitro*. *Acta Biomater.* **7,** 1339–1345
73. Zwaal, R. F., Comfurius, P., and Bevers, E. M. (2005) Surface exposure of phosphatidylserine in pathological cells. *Cell. Mol. Life Sci.* **62,** 971–988
74. Aikawa, E., Nahrendorf, M., Figueiredo, J. L., Swirski, F. K., Shtatland, T., Kohler, R. H., Jaffer, F. A., Aikawa, M., and Weissleder, R. (2007) Osteogenesis associates with inflammation in early-stage atherosclerosis evaluated by molecular imaging *in vivo*. *Circulation* **116,** 2841–2850
75. Grandjean-Laquerriere, A., Laquerriere, P., Guenounou, M., Laurent-Maquin, D., and Phillips, T. M. (2005) Importance of the surface area ratio on cytokines production by human monocytes *in vitro* induced by various hydroxyapatite particles. *Biomaterials* **26,** 2361–2369
76. Nadra, I., Mason, J. C., Philippidis, P., Florey, O., Smythe, C. D., McCarthy, G. M., Landis, R. C., and Haskard, D. O. (2005) Proinflammatory activation of macrophages by basic calcium phosphate crystals via protein kinase C and MAP kinase pathways. A vicious cycle of inflammation and arterial calcification? *Circ. Res.* **96,** 1248–1256
77. Nadra, I., Boccaccini, A. R., Philippidis, P., Whelan, L. C., McCarthy, G. M., Haskard, D. O., and Landis, R. C. (2008) Effect of particle size on hydroxyapatite crystal-induced tumor necrosis factor alpha secretion by macrophages. *Atherosclerosis* **196,** 98–105
78. Shanahan, C. M. (2007) Inflammation ushers in calcification. A cycle of damage and protection? *Circulation* **116,** 2782–2785
79. Jahnen-Dechent, W. (2005) Lot's wife's problem revisited. How we prevent pathological calcification. in *Biomineralization* (Bauerlein, E., ed) pp. 243–267, Wiley, Weinheim, Germany
80. Jahnen-Dechent, W., Heiss, A., Schäfer, C., and Ketteler, M. (2011) Fetuin-A regulation of calcified matrix metabolism. *Circ. Res.* **108,** 1494–1509
81. Jahnen-Dechent, W., Schäfer, C., Ketteler, M., and McKee, M. D. (2008) Mineral chaperones. A role for fetuin-A and osteopontin in the inhibition and regression of pathologic calcification. *J. Mol. Med.* **86,** 379–389
82. Herrmann, M., Schäfer, C., Heiss, A., Gräber, S., Kinkeldey, A., Büscher, A., Schmitt, M. M., Bornemann, J., Nimmerjahn, F., Herrmann, M., Helming, L., Gordon, S., and Jahnen-Dechent, W. (2012) Clearance of fetuin-A-containing calciprotein particles is mediated by scavenger receptor-A. *Circ. Res.* **111,** 575–584
83. Hess, D. J. (1997) *Can bacteria cause cancer?* pp. 7–48, New York University Press, New York
84. Domingue, G. J., Sr., and Woody, H. B. (1997) Bacterial persistence and expression of disease. *Clin. Microbiol. Rev.* **10,** 320–344
85. McLaughlin, R. W., Vali, H., Lau, P. C., Palfree, R. G., De Ciccio, A., Sirois, M., Ahmad, D., Villemur, R., Desrosiers, M., and Chan, E. C. (2002) Are there naturally occurring pleomorphic bacteria in the blood of healthy humans? *J. Clin. Microbiol.* **40,** 4771–4775
86. Wainwright, M. (2010) The overlooked link between non-virus microbes and cancer. *Sci. Prog.* **93,** 393–402
87. Samoylov, A. M., Samoylova, T. I., Pustovyy, O. M., Samoylov, A. A., Toivio-Kinnucan, M. A., Morrison, N. E., Globa, L. P., Gale, W. F., and Vodyanoy, V. (2005) Novel metal clusters isolated from blood are lethal to cancer cells. *Cells Tissues Organs* **179,** 115–124